

## RECENT RESULTS IN T.C.-I UNICAMP

M.Machida\*, E.A.Aramaki\*\*, P. Porto, L.A. Berni, P.H. Sakanaka, M. Ueda\*\*,\*  
Y. Aso\*\*\*.

Instituto de Física Gleb Wataghin, Universidade Estadual de Campinas, 13001,  
SP, Brasil.

Abstract: Recent results obtained in the imollosion phase of the field reversed theta-pinch T.C.-I operating at UNICAMP are present. The diagnostics involved in this phase are: internal and external probes, Rogowski loops, Faraday Cup, photodiode and spectrometer measurements. The main results from these diagnostics are: total current on solenoid coils for 20 kV discharge, 150 kA; maximum magnetic field, 3kG; end scape speed,  $3 \times 10^6$  cm/s; scape beam density,  $2,6 \times 10^{12}$  cm<sup>-3</sup>; estimated ion temperature at the center = 150 eV; line density from MHD oscillations,  $\approx 2 \times 10^{15}$  cm<sup>-3</sup>.

The field reversed theta-pinch T.C.-I operating at Plasma Laboratory, UNICAMP, is a medium size machine with four capacitors bank with crow - bar. It's main objectives are the studies of FRC formation, equilibrium and n=2 instability stabilization by multipole and magnetic divertor effect. As a first step, the formation phase is analysed using external and internal magnetic probes, Rogowski loops, Faraday Cup, photodiode and spectrometer measurements.

The main parameters of the machine are:

a) Main Bank

C = 28  $\mu$ F  $\tau_{rise} = 5 \mu$ s  
V = 20 kV (up to 50 kV)  $\tau_{decay} = 35 \mu$ s  
E = 5.6 kJ (up to 35 kV)  
L = 28 nH  
 $B_z = 3.5$  kG

b) Pre-Heating Bank

C = 1.6  $\mu$ F  $\tau_{rise} = 2 \mu$ s  
V = 25 kV  
E = 0.5 kJ  
L = 370 nH  
B = 0.4 kG

Usually, the pre-heating bank is crow-barred after 2 or 3 oscillations.

c) Bias Bank

C = 440  $\mu$ F                       $\tau_{\text{rise}} = 40 \mu\text{s}$   
V = 2 kV  
E = 0.9 kJ  
L = 1112 nH  
B = 0.5 kG  
No crow-bar.

d) Multipole or Magnetic Divertor Bank

C = 7.4  $\mu$ F                       $\tau_{\text{rise}} = 3 \mu\text{s}$   
V = 25 kV  
E = 2.3 kJ  
L = 75 nH  
B = 2 kG

With crow-bar . This bank is not operational yet.

Besides this values the machine uses:

R.F. generator to pre-heating: 100 W, 30 MHz.

Liquid Ni cooled diffusion pump: base pressure =  $6 \times 10^{-7}$  Torr.

Filling pressure: 5 mTorr, Helium gas.

Solenoid dimensions:

l = 65 cm (length)  
 $\phi_i = 16$  cm (internal diameter)  
 $\phi_m = 15$  cm (minor diameter)  
 $L_0 = 35$  nH (total inductance)

The schematic view of the machine is shown on the figure I. In the figure II we present the discharge sequence taken by external magnetic probes and Rogowski loops. The Rogowski loop rounded on one of the solenoid coils has been calibrated using a Pearson Electronics INC. wide band current transformer, model 411, which gives 24 kA/V on the oscilloscope signal.

The magnetic probe datas have been calibrated using one loop solenoid current and RLC oscillation calculations taken directly from the pictures.

The Faraday Cup measurements have been performed by using single cup, biased system as can be seen on the figure III. It has been used to measure the scape particle from the open ended region for the case with and without FRC formation. As can be seen in the figure IV, in the case of FRC formation, with bias field, the scape beam density is  $2.6 \times 10^{12} \text{ cm}^{-3}$  whereas for the case of no bias field, e.g., no FRC formation, is  $3.6 \times 10^{12} \text{ cm}^{-3}$ .

In the case of fill pressure variation for 5, 10 and 25 mTorr, the best result is obtained for 5 mTorr case where the scrape speed is measured to be  $8 \times 10^6$  cm/s as can be seen on figure V.

The base pressure of the system plays very important role on the FRC formation as can be seen from spectrometer and photodiode measurements. The spectrometry measurements are being done by using a Jarrell Ash one meter Spectrometer, model 78 - 466, to measure the He II (4686 Å) line.

The photodiode set up is used to monitor the bremsstrahlung light emission at the center of the solenoid. The light is collected by a fiber optic cable and sent to the diagnostic room, where a H.P. 466A amplifier is used.

In the figure VI-a is shown the case where the base pressure was poor ( $\sim 6 \times 10^{-5}$  Torr with no liquid Ni trap), the HeII (4686 Å) usually is present at second compression and the bremsstrahlung radiation is also more intense on the second compression (figure VI-b). For the case where the base pressure is  $7 \times 10^{-7}$  Torr as can be seen on the figure VI-c, the situation is inverse, we can notice more HeII line intensity on first time and more bremsstrahlung radiation on the first zero crossing region too (figure VI-d). The best operation regime has been taken as one where HeII emission is the highest with base pressure of  $7 \times 10^{-7}$  Torr.

Another consideration is the time between the pre - heating bank and main bank discharge. Since our system possesses crow-bar on pre-heating bank switch we can vary the time interval between two bank without getting RLC oscillations from pre-heating bank on the main phase. The figure VII shows the case where the time interval was kept at 18  $\mu$ s, and another at 10  $\mu$ s. As can be seen from the spectrometer measurements, the HeII line is more efficient on the  $\Delta t = 10 \mu$ s case.

The typical ion temperature measurement by Doppler broadening of the HeII line shows that the temperature is about 70 eV as can be seen on the figure VIII.

As the conclusion for the FRC formation phase, the T.C.-I best running condition has been determined using electromagnetic probes and optical measurements. The second stage, FRC equilibrium and stability analysis is under operation and no results is available up to this time.

This work has been supported by FINEP, FAPESP and CNPQ.

\* actual address: Instituto de Física, Universidade de São Paulo, SP, Brasil.

\*\* Universidade Estadual Paulista " Júlio de Mesquita Filho" Campus de Guaratinguetã, Faculdade de Engenharia, SP, Brasil.

\*\*\* Ministério de Ciência e Tecnologia, Instituto de Pesquisas Espaciais ( INPE ), São José dos Campos, SP, Brasil.

.352.

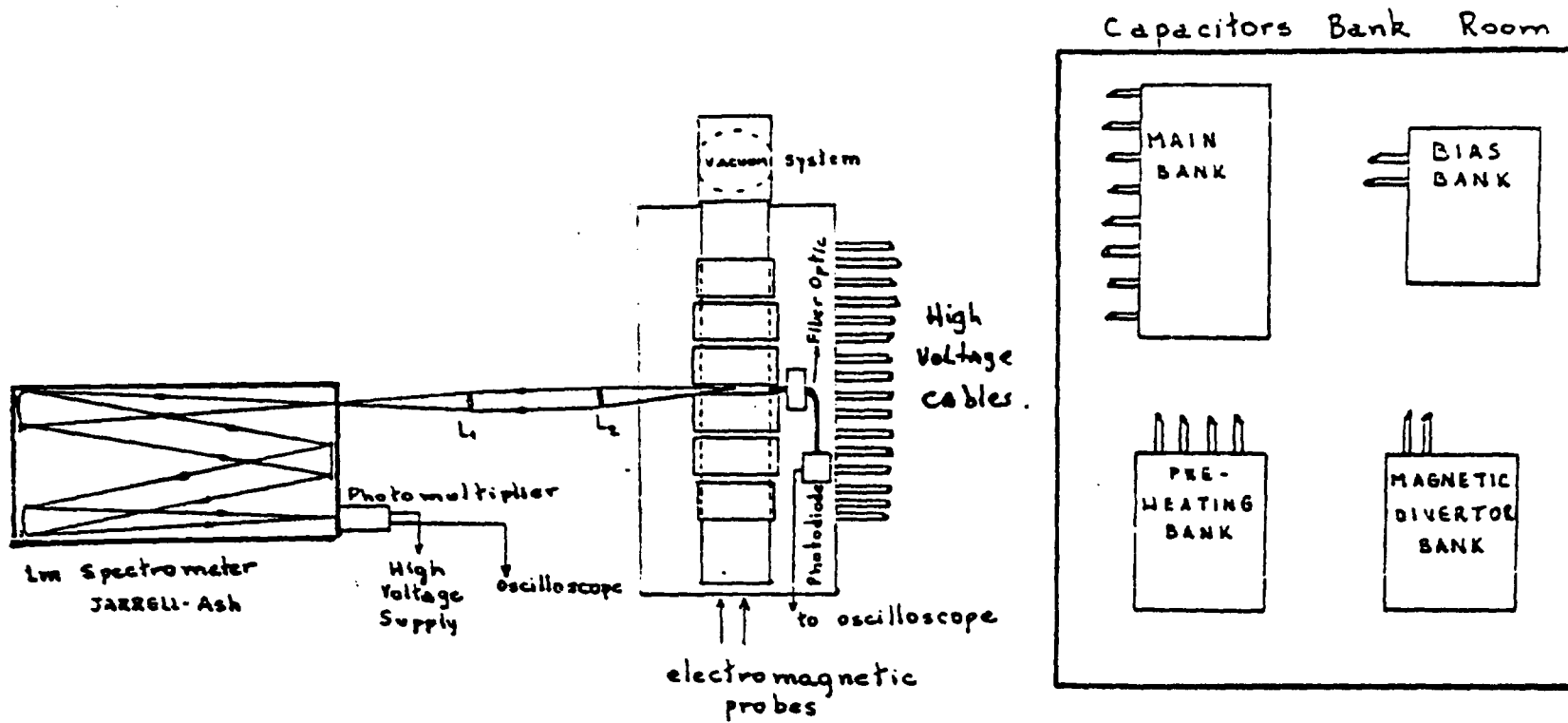
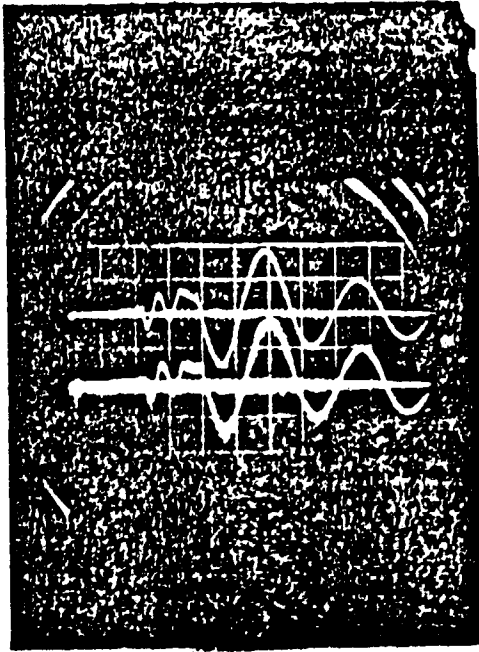


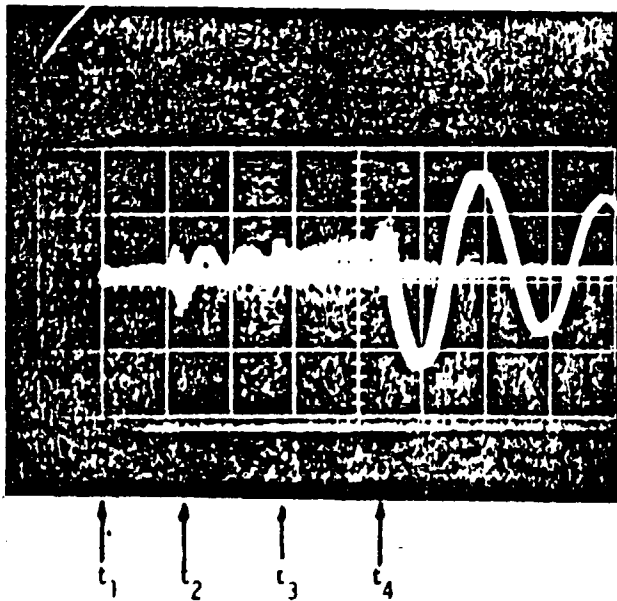
FIGURE I : Schematic view of T.C - I machine.



(a) upper signal:  
 one loop ext. mag. probe  
 hor.: 10  $\mu$ s/div  
 vert.: 0.05 v/div.

(b) lower signal:  
 local ext. mag. probe.  
 hor.: 10  $\mu$ s/div  
 vert.: .5 v/div.

vaccum discharge.

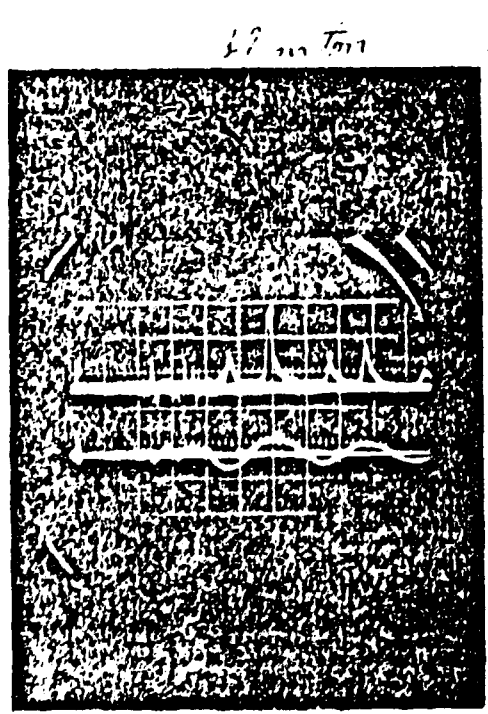
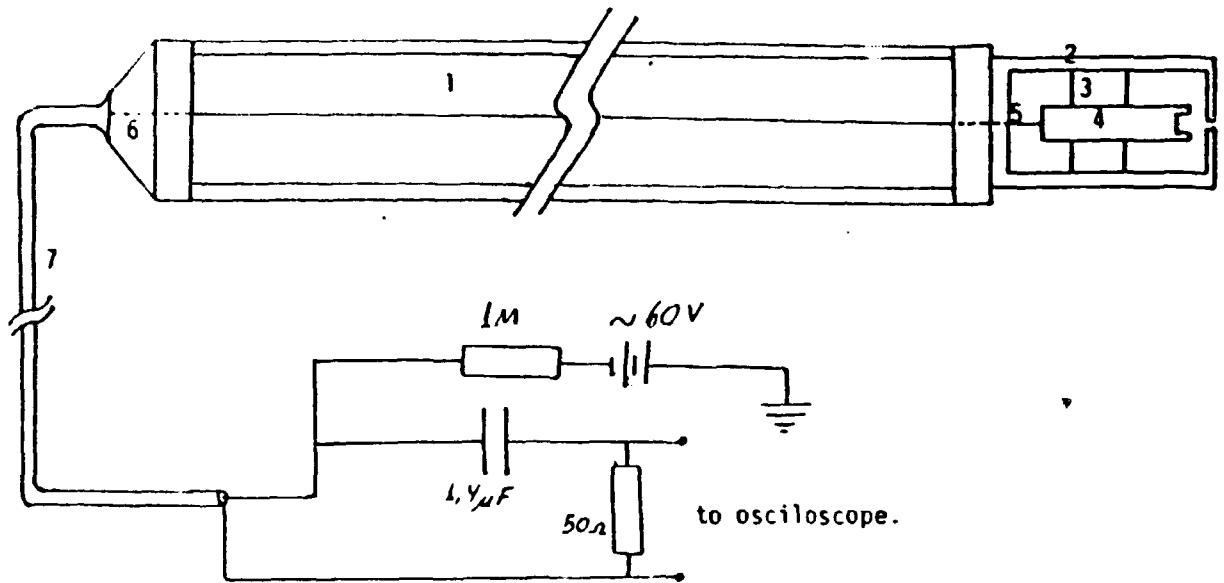


(c) Rogowski loop:

hor.: 10  $\mu$ s/div.  
 vert.: .5 v/div.

$t_1$ : Bias bank.  
 $t_2$ : Pre-heating bank.  
 $t_3$ : Pre-heating C.B.  
 $t_4$ : Main bank.

FIGURE 11: Discharge sequence of the T.C.-I taken by (a),(b) external magnetic probes and (c) Rogowski loop signal on solenoid.  
 Upper and lower signal are distinct discharge with no plasma.

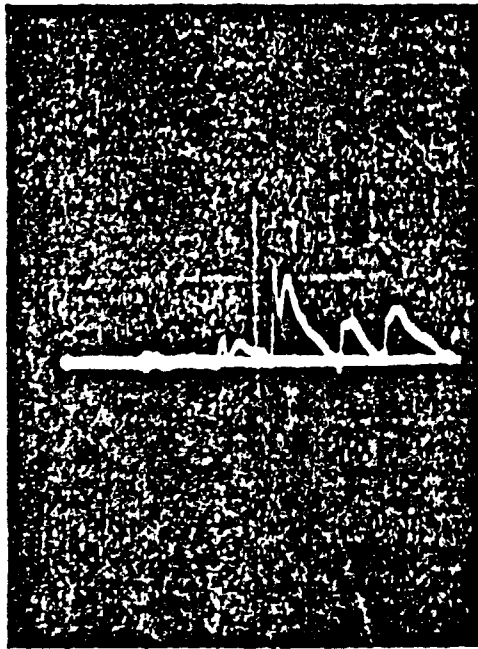


- 1-1.5 m pirex tube.
- 2-copper tube
- 3-insulator(nylon)
- 4-copper collector
- 5-coax. center wire.
- 6-vacuum sealed connector.
- 7-double shielded coax. cable.

upper signal : Faraday Cup  
 vert. : 2v/div.  
 hor. : 10 μs/div.

lower signal: mag. probe signal  
 vert. : .5 v/div.  
 hor. : 10 μs/div.

FIGURE III : Schematic view of the Faraday Cup and typical discharge probe signal.



$T_1$   $T_2$   $T_3$   $T_4$

(a) with bias field.

vert. : .5 v/div.

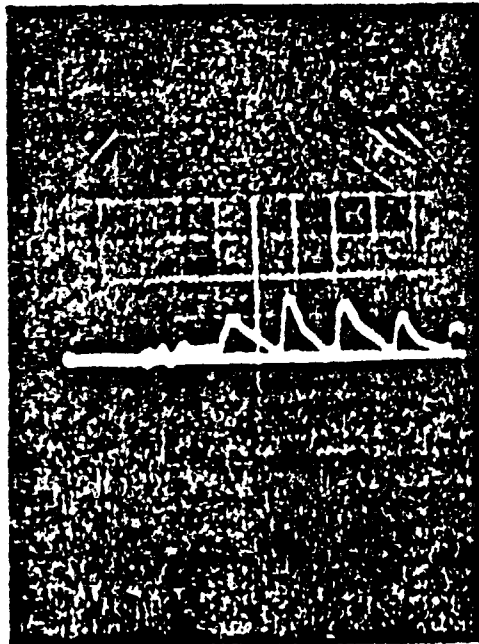
hor. : 10  $\mu$ s/div.

$t_1$  - bias discharge.

$t_2$  - p.heating disch.

$t_3$  - 1st compression  
main disch.

$t_4$  - 2nd compression  
main disch.



$T_1$   $T_2$   $T_3$   $T_4$

(b) with no bias field.

vert. : .5 v/div.

hor. : 10  $\mu$ s/div.

$t_1$  - 0.0 no bias

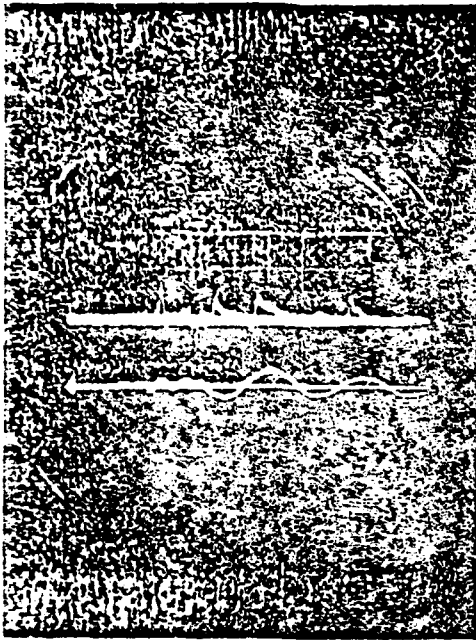
$t_2$  - pre heating disch.

$t_3$  - 1st compression  
main disch.

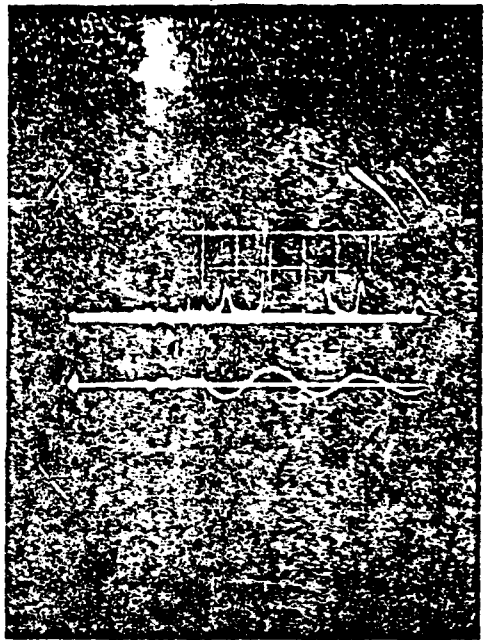
$t_4$  - 2nd. compression  
main disch.

FIGURE IV . Faraday Cup measurements in the case of with and without bias field influence.

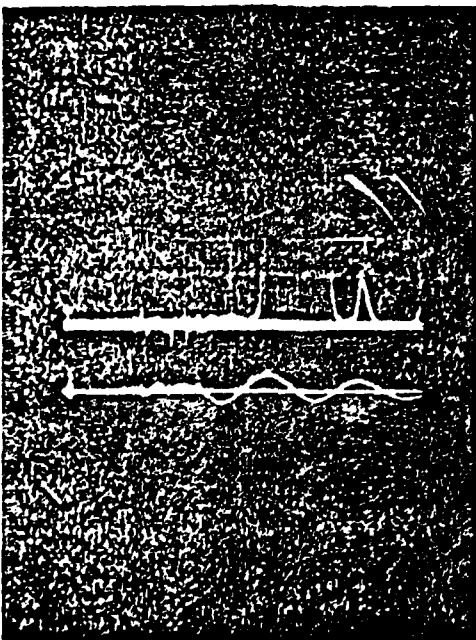




(a)



(b)



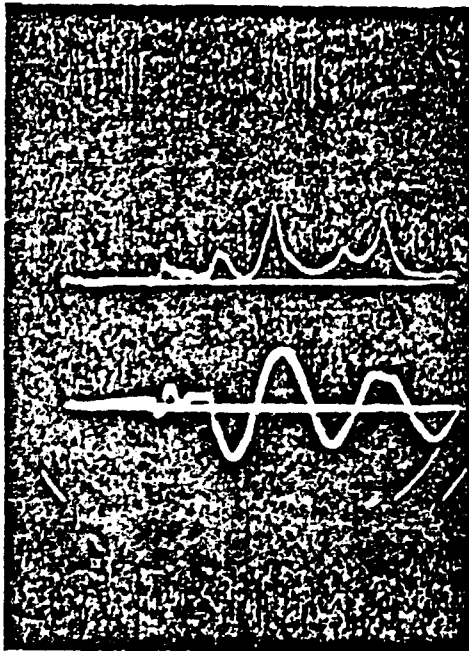
(c)

- (a)- 5 mTorr case
- (b)- 10 mTorr case
- (c)- 25 mTorr case

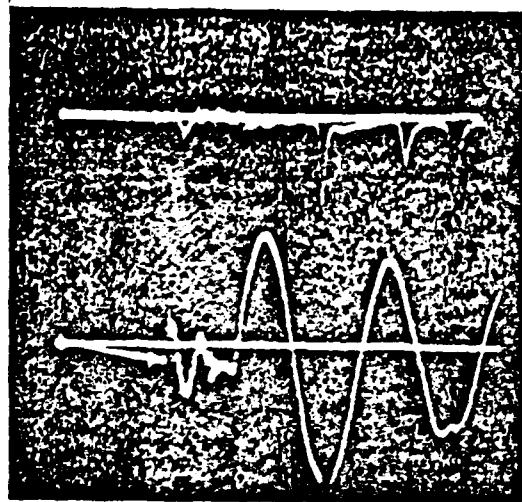
All upper signals- Faraday Cup.  
 vert. : 2v/div.  
 hor. : 10  $\mu$ s/div.

All lower signals-ext. mag. probe  
 vert. : .5 v/div.  
 hor. : 10  $\mu$ s/div.

FIGURE V : Variation of scape particles by filling pressure variation.

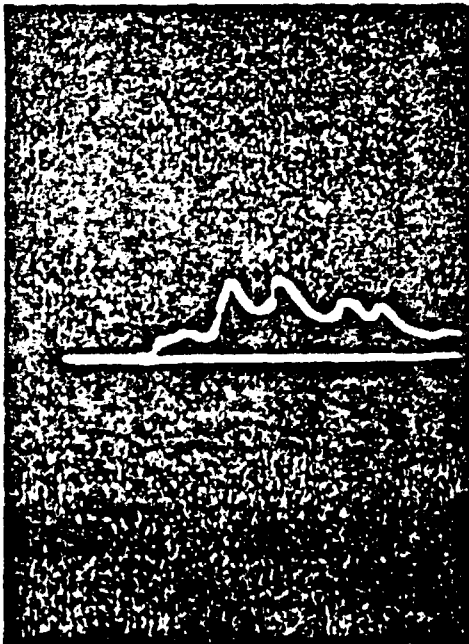


(a) upper line: photodiode: 1 v/div  
 10 μs/div  
 (b) lower line: ext. mag. probe



1 v/div VI-0.5/div

(b) upper signal: He II (4686 Å)  
 vert.: .1 v/div.  
 hor.: 10 μs/div.  
 lower signal: ext. mag. probe.  
 vert.: .5 v/div.  
 case (a) and (b) base pressure =  $6 \times 10^{-5}$  torr

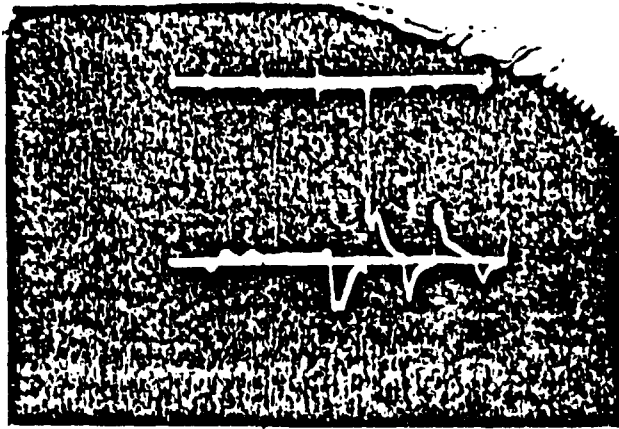


(c) photodiode signal  
 base pressure =  $7 \times 10^{-7}$  torr.



(d) upper signal: He-II (4686 Å).  
 lower signal: internal mag.  
 probe signal (r=2.0 cm).  
 vert.: .2 v/div.  
 hor.: 10 μs/div.

FIGURE VI The effect of the base pressure on the emission intensity.



(a)  
 upper signal: He II (4686 Å).  
 vert. : .5 v/div.  
 hor. : 10 μs/div.  
 lower signal: internal mag.  
 probe ( r = 2.0 cm ).  
 vert. : .2 v/div.  
 hor. : 10 μs/div.

(b) compare with figure VI-d.

$$\Delta t = 10 \mu s.$$

10 μs  
 $\Delta t = 18 \mu s.$

FIGURE VII : The effect of the time interval between pre-heating and main bank discharge timing for He II line emission.

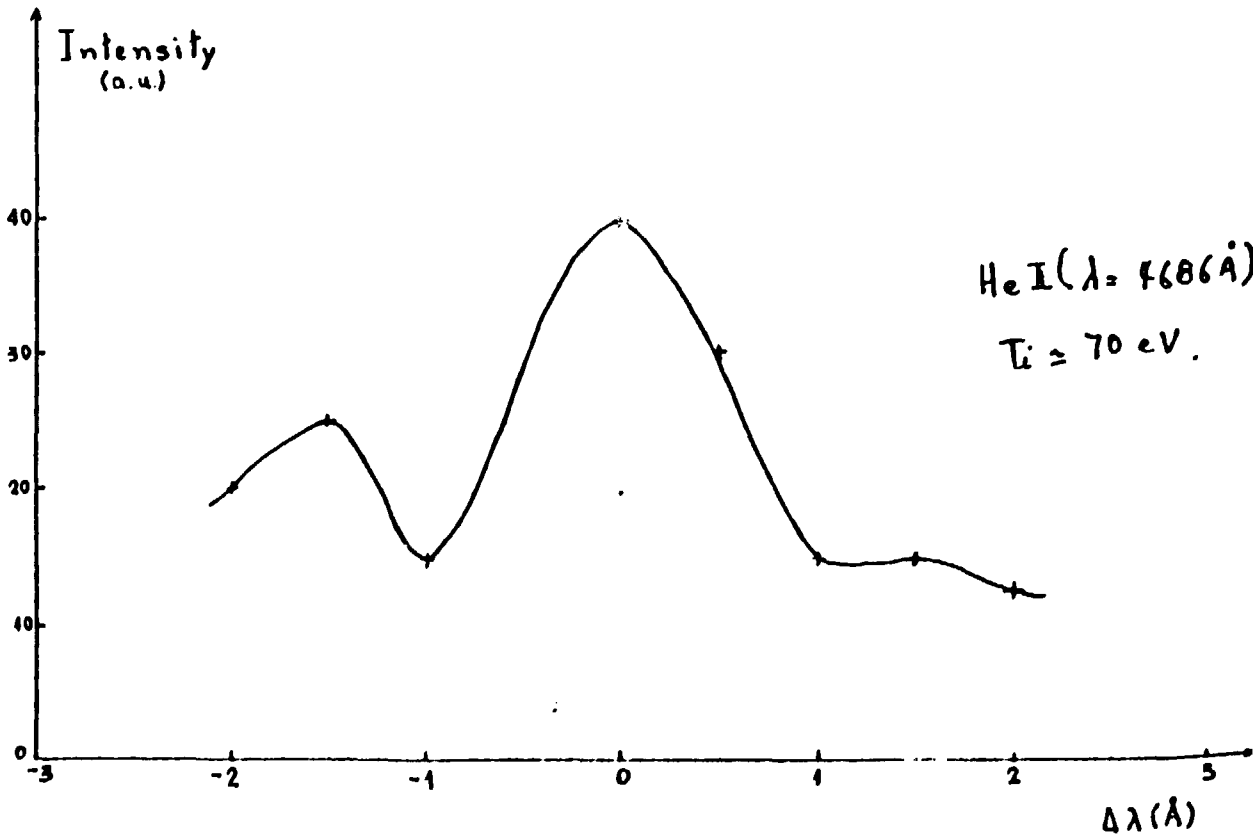


FIGURE VIII : Ion temperature measurement by Doppler broadening of the He II (4686 Å) line.